





## Paraxial skyrmionic beams

Sijia Gao <sup>\*</sup>, Fiona C. Speirits, Francesco Castellucci, Sonja Franke-Arnold , and Stephen M. Barnett <sup>†</sup>  
*School of Physics and Astronomy, University of Glasgow, Glasgow G12 8QQ, United Kingdom*

Jörg B. Götze   
*School of Physics and Astronomy, University of Glasgow, Glasgow G12 8QQ, United Kingdom  
 and College of Engineering and Applied Sciences, Nanjing University, Nanjing 210093, China*



(Received 24 June 2020; accepted 7 October 2020; published 17 November 2020)

We show that a class of vector vortex beams possesses a topological property that derives both from the spatially varying amplitude of the field and its varying polarization. This property arises as a consequence of the inherent skyrmionic nature of such beams and is quantified by the associated skyrmion number. We illustrate this idea for some of the simplest vector beams and discuss the physical significance of the skyrmion number in this context.

DOI: [10.1103/PhysRevA.102.053513](https://doi.org/10.1103/PhysRevA.102.053513)

### I. INTRODUCTION

Recent developments have highlighted the growing utility of structured light, that is, optical fields in which the spatial variation of the field amplitude and/or the polarization are specifically designed for a given task [1–5]. Important examples include the formation of optical beams carrying orbital angular momentum [6–10], polarization or helicity patterns [11–16], and the vector vortex beams and their relatives [17–25]. We show that there is a skyrmion field associated specifically with a class of vector vortex beams and that the associated skyrmion number is readily identified with a simple property of the beam. As such, the skyrmion number provides a natural way to present the variety of possible vector beams. It is noteworthy that this property is explicitly a feature of vector beams: A skyrmion field exists only if both the polarization and the field amplitude are spatially varying. In this sense skyrmion beams are related to the Poincaré beams, in which every possible polarization is to be found at some location in the plane perpendicular to the propagation direction [26]. A skyrmion structure has been observed in Poincaré beams and the relation between skyrmions and coverage of the Poincaré sphere has been examined in Ref. [27]. We find, however, that skyrmion beams are not equivalent to Poincaré beams; all of the skyrmion beams we present here are indeed Poincaré beams, but we present also an example of a Poincaré beam with skyrmion number 0.

Skyrmions were first proposed for the study of mesons [28,29], but the idea has since found wide application in many areas of physics including quantum liquids [30–32], magnetic materials [33–35], two-dimensional (2D) photonic materials [36], and in the study of fractional statistics [37]. Recently, they have been observed in optics by the controlled

interference of plasmon polaritons [38,39]. We show here that a wide range of freely propagating optical beams also possess a nontrivial skyrmion number and with it a skyrmion number, the value of which is simply related to a topological property of the beam.

### II. CONSTRUCTING SKYRMIONIC BEAMS

We consider a paraxial beam of either light [40,41] or electrons [42–44] and express the local polarization or spin direction, respectively, in the form

$$|\Psi(\mathbf{r})\rangle = u_0(\mathbf{r})|0\rangle + e^{i\theta_0}u_1(\mathbf{r})|1\rangle. \quad (1)$$

Here,  $|0\rangle$  and  $|1\rangle$  represent any two orthogonal optical polarization or electron spin states, while  $u_0(\mathbf{r})$  and  $u_1(\mathbf{r})$  are two orthogonal spatial modes [45] and the global phase difference between the two modes is denoted by  $\theta_0$ . That it is always possible to write the spatially varying polarization or spin in this way is a consequence of the Schmidt decomposition, originally introduced in the theory of integral equations [46], but perhaps more familiar from the study of entangled states in quantum theory [47,48]. The skyrmion field and number depend only on the spatial variation of the polarization or spin direction and for this reason it is convenient to work with a locally normalized state in the form

$$|\psi(\mathbf{r})\rangle = \frac{|0\rangle + v(\mathbf{r})|1\rangle}{\sqrt{1 + |v(\mathbf{r})|^2}}, \quad (2)$$

where  $v(\mathbf{r}) = e^{i\theta_0}u_1(\mathbf{r})/u_0(\mathbf{r})$ .

The skyrmion field is most readily defined in terms of an effective magnetization  $\mathbf{M}$ , which is the local direction of the Poincaré vector for light in Fig. 1 or the Bloch vector for an electron beam. In terms of our locally normalized state it is

$$\mathbf{M} = \langle\psi(\mathbf{r})|\boldsymbol{\sigma}|\psi(\mathbf{r})\rangle, \quad (3)$$

where  $\boldsymbol{\sigma}$  is a vector operator with the Pauli matrices as Cartesian components. For a light beam, the Cartesian components

<sup>\*</sup>s.gao.2@research.glasgow.ac.uk

<sup>†</sup>Stephen.Barnett@glasgow.ac.uk

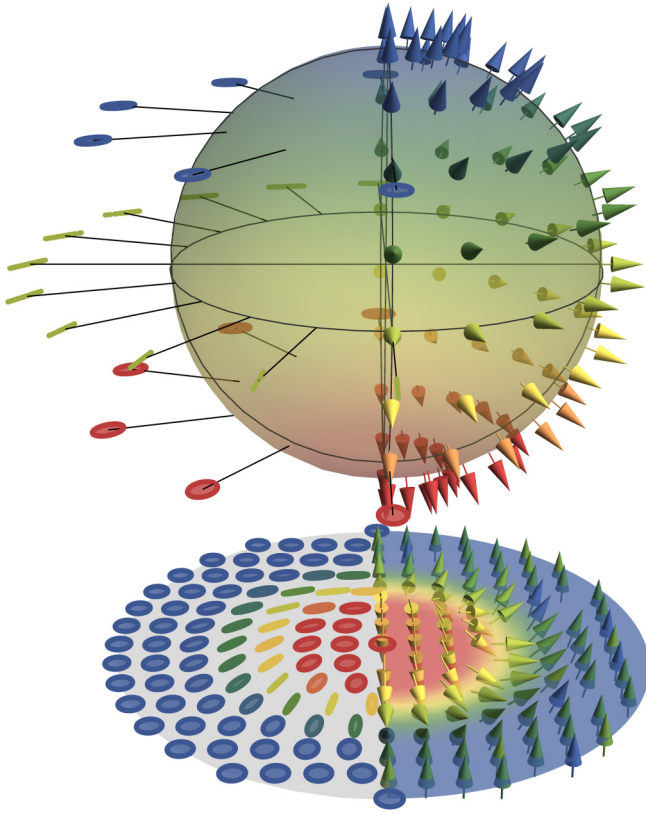


FIG. 1. Stereographic projection of the spatially varying polarization or effective magnetization  $\mathbf{M}$  onto the Poincaré or Bloch sphere. We encode the degree of circular polarization  $S_3$  and the  $z$  component  $M_z$  on the same color scheme. For definiteness we choose in our examples the polarization states  $|0\rangle$  and  $|1\rangle$  to correspond to left- and right-handed circular polarization, respectively, or, for electrons, the eigenstates of the  $z$  component of the spin.

of  $\mathbf{M}$  correspond to the normalized local Stokes parameters  $S_1$ ,  $S_2$ , and  $S_3$  [49], and for the electrons to the local directions of the electron spin. The  $i$ th component of the associated skyrmion field is

$$\Sigma_i = \frac{1}{2} \epsilon_{ijk} \epsilon_{pqr} M_p \frac{\partial M_q}{\partial x_j} \frac{\partial M_r}{\partial x_k}, \quad (4)$$

where  $\epsilon_{ijk}$  is the alternating or Levi-Civita symbol and we employ the summation convention. The form of the skyrmion field ensures that it is transverse ( $\nabla \cdot \Sigma = 0$ ). This means that there are no sources or sinks for the skyrmion field and the associated field lines can only form loops or extend to infinity [50]. It follows that the flux of the skyrmion field through any closed surface is zero,  $\oint \Sigma \cdot d\mathbf{S} = 0$ .

We consider a beam propagating in the  $z$  direction. In each transverse plane of the beam the polarization or spin pattern can form a skyrmion reminiscent of those familiar from the study of magnetic skyrmions. To facilitate this comparison, and also to characterize the variety of skyrmions, we employ the skyrmion number

$$n(z) = \frac{1}{4\pi} \int \Sigma_z dx dy, \quad (5)$$

where the integral runs over the whole of the plane perpendicular to the propagation direction of the beam.

Optical vector vortex beams typically have a spatially varying polarization pattern that originates from the differential orbital angular momentum of the contributing modes [4,18] and exhibit intriguing topological [51–54] and focusing properties [55,56]. We consider the simplest case of such beams in which the two orthogonal modes, with amplitudes  $u_0(\mathbf{r})$  and  $u_1(\mathbf{r})$ , are Laguerre-Gaussian (LG) modes

$$\begin{aligned} u_p^\ell(\rho, \phi, z) = & \sqrt{\frac{2p!}{\pi(p+|\ell|)!}} \frac{1}{w(z)} \left(\frac{\rho\sqrt{2}}{w(z)}\right)^{|\ell|} \exp\left(\frac{-\rho^2}{w^2(z)}\right) \\ & \times L_p^{|\ell|} \left(\frac{2\rho^2}{w^2(z)}\right) e^{i\ell\phi} \exp\left(-i\frac{\rho^2}{w^2(z)} \frac{z-z_0}{z_R}\right) \\ & \times \exp\left[-i(2p+|\ell|+1) \tan^{-1}\left(\frac{z-z_0}{z_R}\right)\right], \end{aligned} \quad (6)$$

familiar from the study of orbital angular momentum [6–10]. Here, we have employed cylindrical polar coordinates  $(\rho, \phi, z)$ ,  $z_R = \pi w_0^2/\lambda$  is the Rayleigh range, and  $w(z) = w_0 \sqrt{1 + (z-z_0)^2/z_R^2}$  is the beam width on propagation. We assume that the modes have the same wavelength  $\lambda$ , but they may differ in the beam parameters  $\ell$ ,  $p$ ,  $w_0$ , and the focal position  $z_0$ . These modes have a vortex of strength  $\ell$  on the  $z$  axis, which is associated with a  $z$  component of the orbital angular momentum of  $\ell\hbar$  per photon (or electron) [6–10]. Modes with different angular momentum numbers  $\ell$  are orthogonal and if we choose two such modes for our two complex amplitudes  $u_0$  and  $u_1$  in (1), then the function  $v(\mathbf{r})$  in (2) for the locally normalized state  $|\psi(\mathbf{r})\rangle$  has the general form

$$v(\mathbf{r}) = f(\rho, z) e^{i\theta(\rho, z)} e^{i\Delta\ell\phi} e^{i\theta_0}, \quad (7)$$

where  $\Delta\ell = \ell_1 - \ell_0$ ,  $f$  and  $\theta$  are real functions of the coordinates  $\rho$  and  $z$ , and  $\theta_0$  incorporates all phase terms. We see that the global phase factor introduced in our original expression, Eq. (1), corresponds in this situation to a rotation of the beam about the  $z$  axis. It is straightforward to calculate the skyrmion field and from this the skyrmion number for our vector vortex beam. We find the simple result that for such beams the skyrmion number is

$$n(z) = \Delta\ell \left( \frac{1}{1 + |v(0, z)|^2} - \frac{1}{1 + |v(\infty, z)|^2} \right). \quad (8)$$

The value of  $n$  is determined solely by which of the two modes  $u_0(\mathbf{r})$  and  $u_1(\mathbf{r})$  dominates on the  $z$  axis, the location of the vortex, and at large distances from the vortex. Unless  $\ell_0 = -\ell_1$ , the ratios  $|v(0, z)|^2$  and  $|v(\infty, z)|^2$  will both be either 0 or  $\infty$ , giving rise to an integer skyrmion number the value of which is determined by which mode dominates at  $\rho = 0$  and at  $\rho = \infty$ . We note that the expression given in Eq. (1) is valid also when  $\ell_0 = -\ell_1$ , but in this case we obtain, typically, a noninteger skyrmion number.

The skyrmionic beams that are simplest to construct comprise a superposition of orthogonal polarization (or spin) states multiplied by  $u_0^\ell$  LG modes with no radial nodes, the same beam width, a common focal point, and with orbital angular momentum differing by one. In this case (7) simplifies

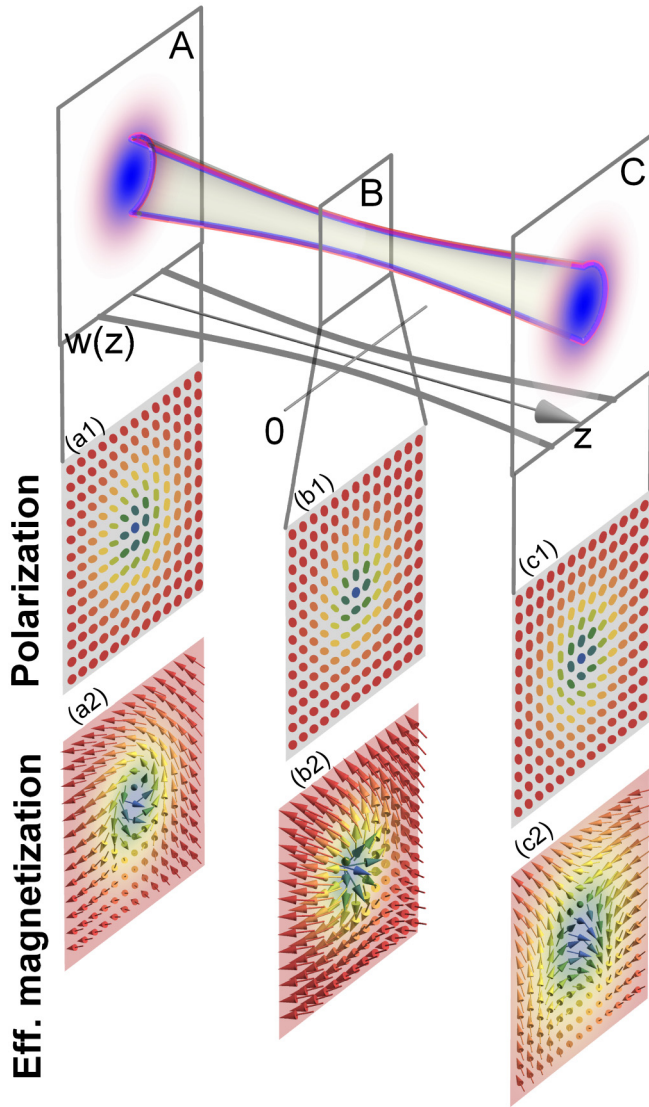


FIG. 2. Polarization structure for a superposition of LG modes with  $\ell_1 = 1$  and  $\ell_0 = 0$  focused at  $z = 0$ . The beam surface separating the regions in which the modes have the larger amplitude,  $u_0$  (blue) and  $u_1$  (red). A, B, and C are three cross sections of interest, at  $z = -10, 0$ , and  $10$  respectively. (a1), (b1), and (c1) are spatially varying polarization patterns corresponding to each plane, while (a2), (b2), and (c2) are the corresponding effective magnetizations, with the classic chiral and hedgehog forms, respectively.

to  $v(\mathbf{r}) = A(z)\rho e^{i\phi}$  (where  $A$  is generally complex) and one polarization dominates at the position of the vortex, with the orthogonal polarization appearing as  $\rho \rightarrow \infty$ . We provide examples for such polarization patterns in Figs. 2(a1) to 2(c1) together with the corresponding effective magnetization in Figs. 2(a2) to 2(c2). The local Bloch vector, representing the local spin direction, is clearly reminiscent of the spiral and hedgehog skyrmions, familiar from the study of magnetic skyrmions [34]; the former arises when  $A$  is imaginary and the latter when the amplitude  $A$  is real.

We note that the natural propagation of the beam will cause the magnetization or polarization pattern to evolve continuously from one of these forms into the other by virtue of the

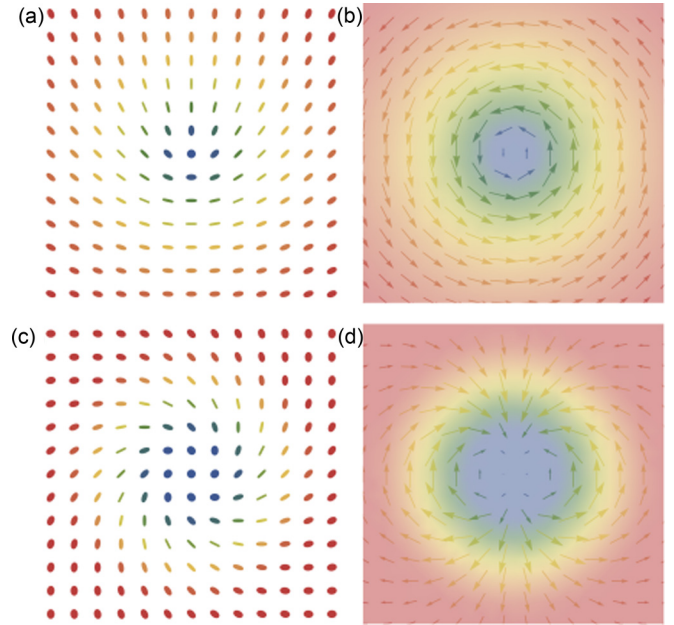


FIG. 3. Comparison of manifestations of spiral skyrmions for polarization and effective magnetization for two different skyrmion numbers  $n = 1$  and  $n = 2$ . (a) A spiraling polarization skyrmion with  $n = 1$ . The full rotation on the Poincaré sphere results in half a rotation for the major axis of the polarization ellipse. (b) The same configuration for the effective magnetization  $\mathbf{M}$ , where the vector describes a full rotation on the Bloch sphere and in the configuration space. (c) As in (a) for  $n = 2$  showing now a full rotation of the polarization. (d) As in (b) for  $n = 2$  showing two full rotations of the effective magnetization.

relative Gouy phase [41], which changes as the beam propagates. The skyrmion number is unchanged, however, taking the value  $+1$  at every transverse plane.

There is, however, a subtle difference in the geometric interpretation between the Poincaré and Bloch sphere. On both spheres, orthogonal states are diametrically opposite. However, for the Poincaré sphere this corresponds to a right angle in the major axes of the polarization, whereas the Bloch vectors of orthogonal states are antiparallel.

We can illustrate the effect of the discrepancy between rotation on the Poincaré sphere and rotation of the polarization ellipse on the geometry of the skyrmion pattern in a comparison between spiral skyrmions formed by superposing LG beams with orbital angular momentum numbers differing by one and two. In Fig. 3 we compare the local polarization ellipse and Bloch vector for a pair of modes with  $\Delta\ell = 1$  (as in Fig. 2) with a pair of modes for which  $\Delta\ell = 2$ . We see that the polarization ellipses and the Bloch vectors rotate as one traverses a path around the vortex. Moreover, along such a path, the polarization ellipse completes half a rotation when  $\Delta\ell = 1$ , whereas the Bloch vector rotates fully. For  $\Delta\ell = 2$  the polarization ellipse completes one full rotation and the Bloch vector winds twice for one complete circle around the vortex.

These are examples of a more general result that for a superposition of modes with a difference in orbital angular momentum number of  $\Delta\ell$ , the Bloch or Poincaré vector

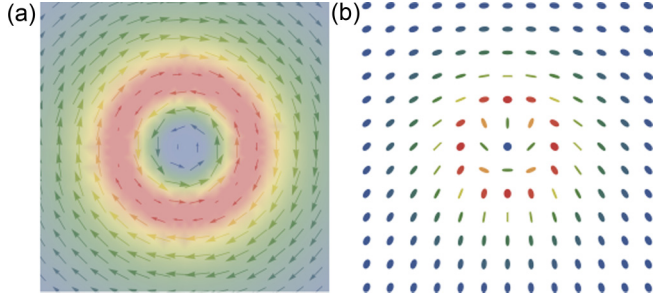


FIG. 4. (a) Magnetization and (b) polarization visualization of a Poincaré beam with skyrmion number 0.

rotates  $\Delta\ell$  times on a path enclosing the vortex. The corresponding polarization ellipse rotates by only half the amount. This behavior persists when we consider modes with radial indices different from zero, although the polarization structure becomes more intricate because of the additional nodal lines. The resulting skyrmion number is nevertheless governed by the difference in dominating behavior described in (8).

The corresponding skyrmion number is  $\Delta\ell$  if the spin or polarization states at the vortex position and at infinity are orthogonal but will be zero if they are the same. This dependence of the skyrmion number on both  $\Delta\ell$  and on the position dependence of the polarization clearly demonstrates that the skyrmion field and number are topological properties of both the spin and orbital angular momenta.

Each of the examples considered so far has a spatially varying polarization or spin that covers the entire Poincaré or Bloch sphere. It follows, therefore, that they are also Poincaré beams and it is natural to ask whether skyrmion beams and Poincaré beams are equivalent. Our final example shows that they are not. Consider a beam formed from orthogonally polarized  $\ell = 1, p = 0$  and  $\ell = 0, p = 1$  modes,

$$|\psi(\mathbf{r})\rangle = \frac{u_1^0(\mathbf{r})|0\rangle + u_0^1(\mathbf{r})|1\rangle}{\sqrt{|u_1^0(\mathbf{r})|^2 + |u_0^1(\mathbf{r})|^2}}, \quad (9)$$

with the amplitudes  $u$  defined in Eq. (6). The effective magnetization and corresponding optical polarization for this beam are depicted in Fig. 4. If we start at the center of the beam and move radially outwards, the changing polarization corresponds to traveling along a great circle on the Poincaré sphere, starting at the north pole and returning to it at infinite distance. Each direction we may choose for our radial path corresponds to a different line of latitude and it is clear, therefore, that we have a Poincaré beam but, because the skyrmion number is zero, it is not a skyrmion beam. It may be that all integer skyrmion beams are also Poincaré beams but further work is needed to determine this.

### III. CONSERVATION OF THE SKYRMION FIELD

The fact that the skyrmion field  $\Sigma$  is divergenceless does not mean that the skyrmion number, defined as the  $z$  component of the flux in (5), is necessarily conserved on propagation. Consider a circular-cylindrical surface of radius  $R$  centered on the position of the vortex extending from  $-z_0$  to  $z_0$ . For the skyrmion field to be divergenceless the flux through all

surfaces of this cylinder has to vanish. The radial flux through the mantle of the cylinder

$$\int_0^{2\pi} d\phi \int_{-z_0}^{z_0} dz \Sigma_\rho = -\Delta\ell \left( \frac{1}{1 + |v(R, -z_0)|^2} - \frac{1}{1 + |v(R, z_0)|^2} \right) \quad (10)$$

is compensated by the flux through the cylinder ends in the  $z$  direction at  $z = -z_0$  and  $z = z_0$ . The expression for these is essentially given by (8), evaluated at  $z = -z_0$  and  $z = z_0$  and  $\rho = R$  instead of infinity. The two terms evaluated at  $\rho = 0$

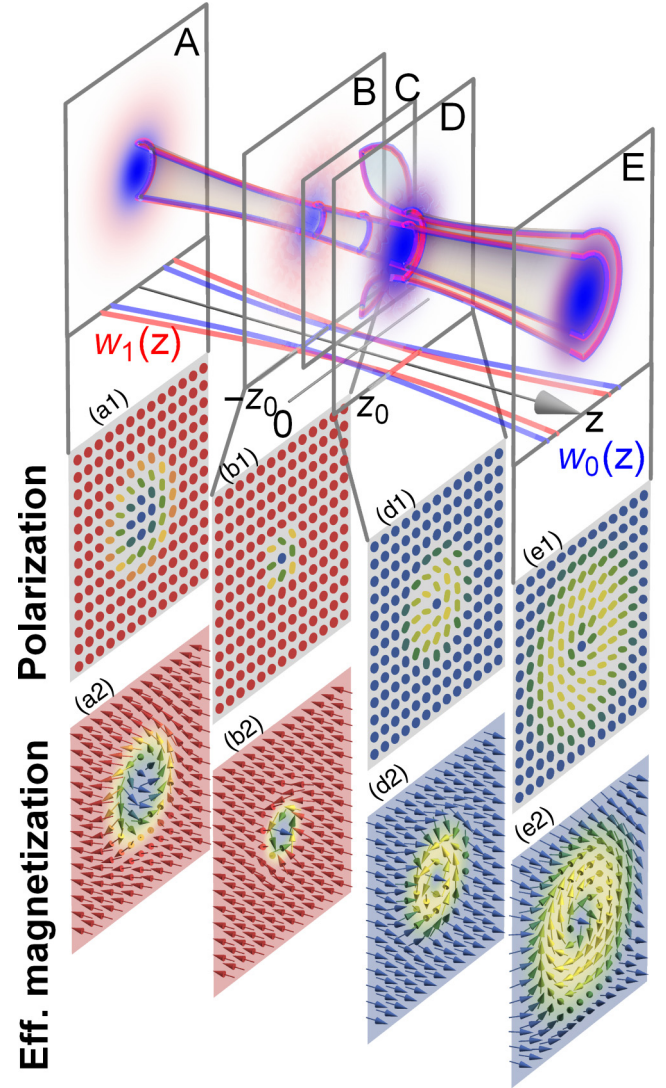


FIG. 5. Polarization structure for the same superposition of modes as in Fig. 2 but focused at different points:  $-z_0 = -2$  and  $z_0 = 2$ . For  $z > 0$  the mode  $u_0$  (blue) has the larger amplitude both in the central region of the beam and the periphery, as indicated by two surfaces of equal amplitude. A, B, D, and E are four cross sections of interest, at  $z = -10, -2, 2, \text{ and } 10$ , respectively. (a1), (b1) and (d1), (e1) are the spatially varying polarization structures showing the qualitative difference for  $z \leq 0$  at those four planes, respectively. (a2), (b2) and (d2), (e2) are the corresponding effective magnetizations with skyrmion number 1 ( $z < 0$ ) and 0 ( $z > 0$ ).

for  $z = -z_0$  and  $z = z_0$  cancel and the total flux through both ends of the cylinder is given by

$$\Delta\ell \left( \frac{1}{1 + |v(R, -z_0)|^2} - \frac{1}{1 + |v(R, z_0)|^2} \right), \quad (11)$$

which is the negative of (10), proving that there is no total flux through the cylinder. If we now construct a superposition of LG beams such that the radial flux is nonvanishing, the flux along the  $z$  direction also needs to be different from zero, which indicates a change in the skyrmion number. The simplest way to demonstrate this is to consider a superposition of LG beams that are focused at different positions along the  $z$  axis. The effect of this is that the polarization behavior at large values of  $\rho$  changes as the beam propagates and the skyrmion number changes from  $\Delta\ell$  to 0 (or from 0 to  $\Delta\ell$ ). This behavior is depicted in Fig. 5, where we see that the polarization at large distances from the central vortex changes abruptly at one transverse plane and with it the skyrmion number. At plane A and B the skyrmion number is +1 and at plane D and E it is equal to zero. The boundary between these two regimes is at plane C, where the skyrmion field lines escape to  $\rho \rightarrow \infty$ . Clearly, this will give a nonzero value for the radial flux because  $|v(R, -z_0)|^2 \neq |v(R, z_0)|^2$  and hence a change in the skyrmion number if we allow  $R$  to tend to infinity.

#### IV. CONCLUSIONS

We have shown that paraxial vector vortex beams, either of light or electrons, possess a topological property that can be identified with a skyrmion number. The associated skyrmion field is transverse (or divergenceless) and this means that there

are no sinks or sources of this field. The skyrmion number for a beam can change on free-space propagation, however, if skyrmion field lines escape radially out of the beam towards regions of negligible intensity. Demonstrating these properties requires the preparation of vector vortex beams and measurement of the polarization or spin in planes perpendicular to the beam axis [57]. We shall report on such experiments elsewhere.

We close by emphasizing that the skyrmionic property of vector beams is distinct from the familiar spin and orbital angular momentum of optical beams [6–10,58]. It is true that the beams we consider here combine optical vortices and polarization, commonly associated with orbital and spin angular momentum, respectively, but the skyrmion number is a topological rather than a mechanical property of the beam. To see this we note that the skyrmion number is unchanged if we apply a global transformation of the polarization, for example, via reflection at a surface or a phase retardation of the constituent beams. On the other hand, we have seen that it is possible for the skyrmion number to change if the two superimposed modes are focused at different propagation distances. The total spin and angular momentum passing through each transverse plane, however, remains unchanged.

#### ACKNOWLEDGMENTS

This work was supported by the Royal Society (RP150122 and RPEA180010), and by the U.K. Engineering and Physical Sciences Research Council (EP/R008264/1) and by the European Training Network ColOpt, funded by the European Union (EU) Horizon 2020 program under the Marie Skłodowska-Curie Action, Grant Agreement No. 721465.

- 
- [1] J. Nye, *Natural Focusing and Fine Structure of Light: Caustics and Wave Dislocations* (Taylor & Francis, London, 1999).
  - [2] J. F. Nye and M. V. Berry, *Proc. R. Soc. London, Ser. A* **336**, 165 (1974).
  - [3] R. Zambrini and S. M. Barnett, *Opt. Express* **15**, 15214 (2007).
  - [4] M. R. Dennis, K. O'Holleran, and M. J. Padgett, in *Progress in Optics*, edited by E. Wolf (Elsevier, Amsterdam, 2009), pp. 293–363.
  - [5] H. Rubinsztein-Dunlop *et al.*, *J. Opt.* **19**, 013001 (2016).
  - [6] L. Allen, M. W. Beijersbergen, R. J. C. Spreeuw, and J. P. Woerdman, *Phys. Rev. A* **45**, 8185 (1992).
  - [7] L. Allen, S. M. Barnett, and M. J. Padgett, *Optical Angular Momentum* (IOP Publishing, London, 2003).
  - [8] A. Bekshaev, M. Soskin, and M. Vasnetsov, *Paraxial Beams with Angular Momentum* (Nova Science, New York, 2008).
  - [9] S. Franke-Arnold, L. Allen, and M. J. Padgett, *Laser Photon. Rev.* **2**, 299 (2008).
  - [10] A. M. Yao and M. J. Padgett, *Adv. Opt. Photon.* **3**, 161 (2011).
  - [11] C. N. Cohen-Tannoudji and W. D. Phillips, *Phys. Today* **43**(10), 33 (1990).
  - [12] J. Dalibard and C. Cohen-Tannoudji, *J. Opt. Soc. Am. B* **6**, 2023 (1989).
  - [13] R. P. Cameron, S. M. Barnett, and A. M. Yao, *New J. Phys.* **14**, 053050 (2012).
  - [14] R. P. Cameron, S. M. Barnett, and A. M. Yao, *J. Mod. Opt.* **61**, 25 (2014).
  - [15] K. C. van Kruining, R. P. Cameron, and J. B. Götte, *Optica* **5**, 1091 (2018).
  - [16] N. Kravets, A. Aleksanyan, and E. Brasselet, *Phys. Rev. Lett.* **122**, 024301 (2019).
  - [17] Q. Zhan, *Adv. Opt. Photon.* **1**, 1 (2009).
  - [18] B. Piccirillo, V. D'Ambrosio, S. Slussarenko, L. Marrucci, and E. Santamato, *Appl. Phys. Lett.* **97**, 241104 (2010).
  - [19] G. Milione, H. I. Sztul, D. A. Nolan, and R. R. Alfano, *Phys. Rev. Lett.* **107**, 053601 (2011).
  - [20] G. Milione, S. Evans, D. A. Nolan, and R. R. Alfano, *Phys. Rev. Lett.* **108**, 190401 (2012).
  - [21] V. D'Ambrosio, E. Nagali, S. P. Walborn, L. Aolita, S. Slussarenko, L. Marrucci, and F. Sciarrino, *Nat. Commun.* **3**, 961 (2012).
  - [22] B. Ndagano, H. Sroor, M. McLaren, C. Rosales-Guzmán, and A. Forbes, *Opt. Lett.* **41**, 3407 (2016).
  - [23] C. Alpmann, C. Schlickriede, E. Otte, and C. Denz, *Sci. Rep.* **7**, 8076 (2017).
  - [24] N. Radwell, R. D. Hawley, J. B. Götte, and S. Franke-Arnold, *Nat. Commun.* **7**, 10564 (2016).
  - [25] C. Rosales-Guzmán, N. Bhebhe, and A. Forbes, *Opt. Express* **25**, 25697 (2017).

- [26] A. M. Beckley, T. G. Brown, and M. A. Alonso, *Opt. Express* **18**, 10777 (2010).
- [27] S. Donati, L. Dominici, G. Dagvadori, D. Ballarini, M. De Giorgi, A. Bramanti, G. Gigli, Y. Rubo, M. H. Szymańska, and D. Sanvitto, *Proc. Natl. Acad. Sci. USA* **113**, 14926 (2016).
- [28] T. H. R. Skyrme, *Proc. R. Soc. London, Ser. A* **260**, 127 (1961).
- [29] T. H. R. Skyrme, *Nucl. Phys.* **31**, 556 (1962).
- [30] D. Vollhardt and P. Wolfe, *The Superfluid Phases of Helium 3* (Dover, New York, 2013).
- [31] G. Volovik and O. U. Press, *The Universe in a Helium Droplet* (Clarendon Press, Oxford, UK, 2003).
- [32] A. Leggett, *Quantum Liquids: Bose Condensation and Cooper Pairing in Condensed-Matter Systems* (Oxford University Press, Oxford, UK, 2006).
- [33] S. Sachdev, *Quantum Phase Transitions* (Cambridge University Press, Cambridge, UK, 2011).
- [34] S. Seki and M. Mochizuki, *Skyrmions in Magnetic Materials* (Springer, Berlin, 2015).
- [35] M. R. Dennis, *Opt. Lett.* **36**, 3765 (2011).
- [36] T. V. Mechelen and Z. Jacob, *Opt. Mater. Express* **9**, 95 (2019).
- [37] F. Wilczek, *Fractional Statistics and Anyon Superconductivity* (World Scientific, Singapore, 1990).
- [38] S. Tsesses, E. Ostrovsky, K. Cohen, B. Gjonaj, N. H. Lindner, and G. Bartal, *Science* **361**, 993 (2018).
- [39] L. Du, A. Yang, A. V. Zayats, and X. Yuan, *Nat. Phys.* **15**, 650 (2019).
- [40] D. Marcuse, *Light Transmission Optics* (Van Nostrand Reinhold, New York, 1989).
- [41] A. Siegman, *Lasers* (University Science Books, Mill Valley, CA, 1986).
- [42] A. El-Kareh and J. El-Kareh, *Electron Beams, Lenses, and Optics*, Vol. 2 (Elsevier, Amsterdam, 2016).
- [43] O. Klemperer and M. Barnett, *Electron Optics* (Cambridge University Press, Cambridge, UK, 1971).
- [44] P. Hawkes, *Electron Optics and Electron Microscopy* (Taylor & Francis, London, 1972).
- [45] We have used a quantum mechanical notation as this aids the analysis to come, but our results apply both to classical and quantum states of light and also to electron beams.
- [46] E. Schmidt, *Math. Ann.* **63**, 433 (1907).
- [47] A. Ekert and P. L. Knight, *Am. J. Phys.* **63**, 415 (1995).
- [48] S. M. Barnett, *Quantum Information* (Oxford University Press, Oxford, 2009).
- [49] M. Born and E. Wolf, *Principles of Optics: Electromagnetic Theory of Propagation, Interference and Diffraction of Light*, 7th ed. (Cambridge University Press, Cambridge, UK, 2000).
- [50] This property is familiar from the study of electric and magnetic fields  $\mathbf{E}$  and  $\mathbf{B}$  in free space. We note, however, that  $\mathbf{\Sigma}$  for light is a nonlinear function of  $\mathbf{E}$  and  $\mathbf{B}$  and so its transverse nature is not simply a consequence of  $\nabla \cdot \mathbf{E} = 0 = \nabla \cdot \mathbf{B}$ .
- [51] I. Freund, *Opt. Commun.* **283**, 1 (2010).
- [52] D. Foster, C. Kind, P. J. Ackermann, J.-S. B. Tai, M. R. Dennis, and I. I. Smalyukh, *Nat. Phys.* **15**, 655 (2019).
- [53] I. Freund, *Opt. Lett.* **36**, 4506 (2011).
- [54] T. Bauer, P. Banzer, E. Karimi, S. Orlov, A. Rubano, L. Marrucci, E. Santamato, R. Boyd, and G. Leuchs, *Science* **347**, 964 (2015).
- [55] Q. Zhan and J. Leger, *Opt. Express* **10**, 324 (2002).
- [56] R. Dorn, S. Quabis, and G. Leuchs, *Phys. Rev. Lett.* **91**, 233901 (2003).
- [57] A. Selyem, C. Rosales-Guzmán, S. Croke, A. Forbes, and S. Franke-Arnold, *Phys. Rev. A* **100**, 063842 (2019).
- [58] S. M. Barnett, L. Allen, R. P. Cameron, C. R. Gilson, M. J. Padgett, F. C. Speirits, and A. M. Yao, *J. Opt.* **18**, 064004 (2016).